# KIAS Lectures on Symplectic Aspects of Degenerations

Jonny Evans

June 24, 2019

This is a series of three lectures I gave at the Korea Institute of Advanced Study in June 2019 at a workshop about "Algebraic and Symplectic Aspects of Degenerations of Complex Surfaces". I will focus on the symplectic aspects, in particular on the case of cyclic quotient surface singularities.

I would like to thank the Korea Institute for Advanced Study for their hospitality during this conference, and acknowledge the support of the Engineering and Physical Sciences Research Council (EPSRC) in carrying out the research which forms the focus of my lectures.

# 1 Lecture 1

## 1.1 Hunting for singularities

Suppose that someone hands you a variety $X$, and asks you to classify degenerations in which $X$ appears as a smooth fibre. This is an extremely difficult question. In this first lecture, I want to convince you that symplectic topology can help you to rule out some possible degenerations. In the same way that a hunted animal leaves footprints as it flees, a singularity sometimes leaves behind a noticeable trace in the smooth fibres of a degeneration, a trace which is visible to symplectic geometry.

### 1.1.1 Degenerations and symplectic parallel transport

What do I mean by a degeneration in this context? I mean a flat family $\pi\colon \mathcal{X} \to \Delta$ over the disc whose fibres $X_s = \pi^{-1}(s)$ are projective varieties. In fact, I'll assume for simplicity:

- that the only singular fibre is $X_0$, and that $X_0$ has a unique isolated singularity $x_0$ (this is just for convenience),

- that $\mathcal{X}$ is smooth away from $x_0$ (but will usually be singular at $x_0$).

More importantly, I want to assume:

- that the fibres $X_s$ are projective subvarieties of the same projective space; in other words that we have a morphism $f\colon \mathcal{X} \to \mathbf{CP}^N$ such that $f_s := f|_{X_s}\colon X_s \to \mathbf{CP}^N$ is an embedding for all $s \in \Delta$ (for example, coming from a relatively ample line bundle on $\mathcal{X}$).

It is this last point which allows us to make the connection with symplectic geometry: the Fubini-Study form $\omega_{FS}$ on $\mathbf{CP}^N$ pulls back to give a symplectic form $\omega_s = f_s^*\omega_{FS}$ on the smooth locus of each fibre $X_s$.

**Lemma 1.1.** *The smooth fibres are all* symplectomorphic. *More precisely, given a path $\gamma\colon [0,1] \to \Delta$ avoiding $0 \in \Delta$, there is a diffeomorphism $\phi_t\colon X_{\gamma(0)} \to X_{\gamma(t)}$ for all $t \in [0,1]$ such that $\phi_t^*\omega_{\gamma(t)} = \omega_{\gamma(0)}$.*

*Proof.* We construct $\phi_t$ as the parallel transport map for a connection on the fibre bundle $\mathcal{X} \setminus X_0 \to \Delta \setminus \{0\}$. The connection is defined as follows. Let $\Omega = f^*\omega_{FS}$. This is a closed (not necessarily nondegenerate[1]) 2-form on $\mathcal{X} \setminus \{x_0\}$. Define the horizontal space at $x \in X_s$ to be

$$\mathcal{H}_x = \{v \in T_x\mathcal{X} \ : \ \Omega(v,w) = 0 \ \forall w \in T_xX_s\}.$$

This is the $\Omega$-orthogonal complement to the vertical tangent space $T_xX_s$, which is indeed complementary to $T_xX_s$ because $X_s$ is a symplectic submanifold with respect to $\Omega$ ($\Omega$ pulls back to $\omega_s$ on $X_s$). The proof that parallel transport with respect to this connection is a symplectic map can be found in [13, Lemma 6.18]. □

Now suppose that $\gamma(1) = 0$ and $\gamma(t) \neq 0$ for $t < 1$. The symplectic parallel transport maps $\phi_t\colon X_{\gamma(0)} \to X_{\gamma(t)}$ are defined for $t < 1$. We would like to define $\phi_1\colon X_{\gamma(0)} \to X_0$ by

$$\phi_1(x) = \lim_{t\to 1} \phi_t(x).$$

**Lemma 1.2.** *This map $\phi_1$ is well-defined.*

*Proof.* Since $\mathcal{X}$ is compact, any sequence $\phi_{t_i}(x)$, $t_i \in [0,1]$ has a convergent subsequence and if $t_i \to 1$ then the limit is in the fibre $X_0$. Pick a convergent subsequence and define $\phi_1(x)$ to be the limit. We need to show that this limit is independent of the choice of convergent subsequence.

Suppose the limit $y = \lim \phi_{t_i}(x)$ of some subsequence is a smooth point of $X_0$. In this case, the horizontal space is still well-defined at $y$, and if we look in a neighbourhood of $y$ then the parallel transport problem (an ordinary differential equation) is well-posed. In particular, the only way this can happen is if $\phi_t(x)$ for

[1] For example, suppose you have a pencil of hypersurfaces in $\mathbf{CP}^N$. If you blow up the base locus, this will separate out the fibres, and give you a degeneration. However, the pullback of the Fubini-Study form along the blow-up is degenerate along the exceptional locus.

$t \in [1-\epsilon, 1]$ is a solution of the parallel transport ODE on this neighbourhood. In that case, by uniqueness of solutions to ODEs, any other subsequence will converge to the same limit point $y$.

The only other possibility is that no subsequence converges to a smooth point, in which case every subsequence converges to $x_0$ (because there's only one singularity by assumption). □

In more general contexts, for example with several singularities or even nonisolated singularities, you could use prove the existence of this map $\phi_1$ using more sophisticated arguments involving Łojasiewicz's inequality (for example, this approach is taken by Harada and Kaveh in their work on toric degenerations).

### 1.1.2 Signs left by singularities

We now use the map $\phi_1 \colon X_{\gamma(0)} \to X_0$ to find objects in the smooth fibre $X_{\gamma(0)}$ which are signs that the singularity is present in $X_0$. The three signs we look for are: the *vanishing cycle*, the *link* and the *Milnor fibre*.

**Definition 1.3** (Vanishing cycle)**.** Let $V := \{x \in X_{\gamma(0)} \ : \ \phi_1(x) = x_0\}$. This is called the *vanishing cycle* of the singularity (with respect to the path $\gamma$).

*Remark* 1.4. There is no *a priori* reason for the vanishing cycle to be nice, e.g. a submanifold or cell complex. It will often turn out in practice to be a Lagrangian cell complex, that is a cell complex of dimension $\frac{1}{2}\dim X$ on which the symplectic form vanishes.

**Definition 1.5** (Link)**.** Let $S_\epsilon \subset \mathbf{CP}^N$ be the sphere of radius $\epsilon$ centred at $f(x_0)$ and let $L_\epsilon = f_0^{-1}(S_\epsilon^{2N+1}) \cap X_0$. For sufficiently small $\epsilon$, $L_\epsilon$ is a contact-type hypersurface called the *link* of $x_0$.

*Remark* 1.6. Recall that a hypersurface $M$ of a $2n$-dimensional symplectic manifold is said to be of *contact type* if there exists a 1-form $\lambda$ on a neighbourhood of $M$ such that $\omega = d\lambda$ on this neighbourhood and such that $\lambda \wedge \underbrace{d\lambda \wedge \cdots \wedge d\lambda}_{n-1}$ is a nowhere vanishing $(2n-1)$-form on $M$ (the pullback of $\lambda$ to $M$ is called a *contact form*).

**Lemma 1.7.** *There is a contact-type hypersurface $M := \phi_1^{-1}(L_\epsilon) \subset X_{\gamma(0)}$ which is contactomorphic to the link of $x_0$.*

*Proof.* The map $\phi_1$ restricts to give a map $X_{\gamma(0)} \setminus V \to X_0 \setminus \{x_0\}$. While $\phi_1$ is only continuous, this restriction is smooth. This is because it is defined as the time 1 map of an ordinary differential equation (the parallel transport problem) which is well-posed wherever the horizontal spaces are well-defined (in particular anywhere except $x_0$). The argument from [13, Lemma 6.18] carries through and shows that it is symplectic. Therefore, as $L_\epsilon$ is disjoint from $x_0$,

$M := \phi_1^{-1}(L_\epsilon)$ is still a contact-type hypersurface in $X_{\gamma(0)}$ and $(\phi_1)|_M$ is the desired contactomorphism to $L_\epsilon$. □

**Definition 1.8** (Milnor fibre)**.** The contact-type hypersurface $M$ divides $X_{\gamma(0)}$ into two regions: a region $W$ containing the vanishing cycle $V$ and its complement. The region $W$ is called the *Milnor fibre* of the singularity. It is a codimension zero symplectic submanifold which is mapped via $\phi_1$ onto a neighbourhood of $x_0$.

*Remark* 1.9. We will often be slightly vague about Milnor fibres. If someone tells you they have found a symplectically embedded ball in a manifold, you should ask them: how big a ball? Balls of different radii are not symplectomorphic (they have different volumes) and there are extremely subtle questions about how big a ball you can embed in a given manifold. Similarly, just because you find two singularities which are locally analytically equivalent, the Milnor fibres you find may not be symplectomorphic: what will be true instead is that you can find inside each of them a common smaller subset. Said another way, the Milnor fibres of two analytically equivalent isolated singularities will have symplectomorphic *completions* (if you attach an infinite cylindrical end); see [2, Proposition11.22]. Apart from in Lemma 3.15, we will ignore these subtle quantitative questions as they have little bearing on what we want to say, and always allow ourselves to pass to a smaller neighbourhood of the vanishing cycle if necessary, using the same notation for a Milnor fibre and its completion.

## 1.2 Cyclic quotient singularities

We now take a concrete example, and identify the link, the Milnor fibre and the vanishing cycle. Let $G$ be the cyclic group of $n$th roots of unity and let $\mu \in G$ act on $\mathbf{C}^2$ (coordinates $(x, y)$) via

$$(x, y) \mapsto (\mu x, \mu^a y),$$

where $a$ is an integer coprime to $n$. The quotient $\mathbf{C}^2/G$ by this group action has an isolated singularity at the origin, which we call the *cyclic quotient singularity of type* $\frac{1}{n}(1, a)$. We will say that $X_0$ has a singularity $x_0$ of this type if $x_0$ has a neighbourhood (in the Euclidean topology) which is biholomorphic to a neighbourhood of $0 \in \mathbf{C}^2/G$.

### 1.2.1 The link

The unit sphere in $\mathbf{C}^2$ is preserved by the action of $G$ and the quotient of the sphere by this action is a 3-manifold called a *lens space* $L(n, a)$. This means that the link of the $\frac{1}{n}(1, a)$ singularity is such a lens space. Therefore if you have a smooth variety $X$ which does not contain any contact-type hypersurfaces

contactomorphic[2] to $L(n,a)$ then it does not admit any degenerations with $\frac{1}{n}(1,a)$ singularities.

### 1.2.2 Milnor fibre

Cyclic quotient singularities can have different smoothings, so there can be several different possible Milnor fibres to look out for. The smoothings were classified by Kollár and Shepherd-Barron [11] and we will discuss this in Section 2.2. In the meantime, we will focus on a specific, important class of examples.

**Definition 1.10** (T-singularities)**.** A cyclic quotient singularity is called a T-singularity if it is of the form $\frac{1}{dp^2}(1, dpq-1)$ with $\gcd(p,q)=1$.

*Remark* 1.11. These are precisely the cyclic quotient singularities admitting a $\mathbf{Q}$-Gorenstein smoothing with terminal total space, hence the name "T".

Fix a T-singularity $\frac{1}{dp^2}(1, dpq-1)$. If we define the semi-invariants

$$u = x^{dp}, \quad v = y^{dp}, \quad w = xy$$

then:

- $uv = w^p$
- under the action of $\mu \in G$,

$$(u,v,w) \mapsto (\mu^{dp}u, \mu^{-dp}v, \mu^{dpq}w)$$

(e.g. $y^{dp} \mapsto (\mu^{dpq-1}y)^{dp} = \mu^{-dp}y^{dp}$ because $\mu^{d^2p^2q} = 1$).

In fact, we get

$$\mathbf{C}[x,y]^G = \mathbf{C}[u,v,w]^{G'}/(uv = w^{dp}),$$

where $G'$ is the cyclic group of order $p$ generated by $\mu^{dp}$. The family of varieties

$$X_s := \{(u,v,w) \in \mathbf{C}^3 \ : \ uv = (w^p - s)(w^p - 2s)\cdots(w^p - ds)\}/G'$$

is therefore a smoothing of $\frac{1}{dp^2}(1, dpq-1)$ (here $G'$ acts with weights $1, -1, q$ on $u, v, w$ respectively, and $s$ is the smoothing parameter).

*Remark* 1.12. Note that the action of $G'$ on $uv = (w^p - s)(w^p - 2s)\cdots(w^p - ds)$ is free, so $X_s$ is a smooth variety.

**Definition 1.13.** We define the manifold $B_{d,p,q}$ to be the symplectic manifold underlying the affine variety $X_1$ (we could take any $X_s$, $s \neq 0$, as they are all symplectomorphic by parallel transport). This is (the symplectic completion of) the Milnor fibre of the cyclic quotient singularity $\frac{1}{dp^2}(1, dpq-1)$.

[2] We equip $L(n,a)$ with the contact structure it inherits as a quotient of the standard contact structure on $S^3$.

*Remark* 1.14. Momentarily, we will study the vanishing cycle and show that it is a Lagrangian cell complex (i.e. a 2-dimensional cell complex on which the symplectic form vanishes) which comprises a chain of $d-1$ Lagrangian spheres attached to a certain immersed Lagrangian disc called a *pinwheel*. Indeed, $B_{d,p,q}$ deformation retracts onto the vanishing cycle, which tells us that

$$H_1(B_{d,p,q};\mathbf{Z}) = \mathbf{Z}/p, \qquad H_2(B_{d,p,q};\mathbf{Z}) = \mathbf{Z}^{d-1}.$$

In the applications below, we are most interested in the case $d = 1$ as the Milnor fibre is then a rational homology ball, so it can be difficult to rule out its appearance on purely topological grounds. In this case, we write $B_{p,q} := B_{1,p,q}$.

### 1.2.3 Vanishing cycle

**Definition 1.15.** Consider the map $S^1 \to S^1$, $z \mapsto z^p$. The cell complex obtained by attaching a 2-cell to $S^1$ using this as the attaching map is called a *pinwheel*. Here is picture indicating how to identify segments of the boundary of the disc to get a pinwheel (for example, when $p = 2$, this is the usual picture of $\mathbf{RP}^2$ as a disc with opposite pairs of points on the boundary identified).

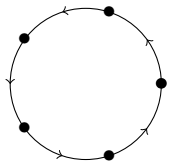

**Proposition 1.16.** *Let $\gamma(t) = 1 - t$. The vanishing cycle associated to $\gamma$ in $B_{d,p,q} = X_1$ is a cell complex comprising a chain of $d-1$ Lagrangian spheres attached to a Lagrangian pinwheel.*

Here, *Lagrangian* means that the symplectic form $\omega_1$ evaluates to zero on pairs of tangent vectors to 2-cells in the vanishing cycle. The rest of this section will be spent justifying this claim.

Consider the projection

$$B_{d,p,q} \to \mathbf{C}, \qquad (u,v,w) \mapsto w^p. \tag{1}$$

This is a holomorphic map whose general fibre is a conic $uv =$ constant. It has the following singular fibres:

- over $w^p = 1, 2, 3, \ldots, d$ there are nodal conics $uv = 0$;
- over $w^p = 0$ the fibre is a smooth conic but it is not reduced: it is the quotient by $G'$ of $\{uv = d!\}$. The generic fibre collapses $p$-to-1 onto this fibre.

In the figure below we indicate these singular fibres.

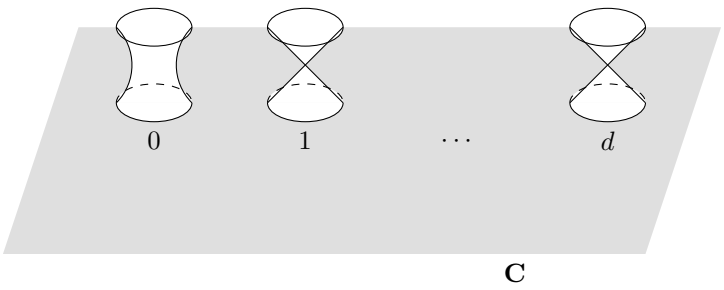


The following lemma gives a way to construct Lagrangian submanifolds in the total space of a conic fibration (or more general degeneration) from Lagrangians in the fibres. We also state and prove the (trickier) converse because we will use it later.

**Lemma 1.17.** *Suppose $\pi\colon \mathcal{Y} \to \mathbf{C}$ is a degeneration/conic fibration and that $\Omega$ is a closed 2-form on $\mathcal{Y}$ whose pullback to fibres of $\pi$ is nondegenerate. Let $\gamma\colon [0,1] \to \mathbf{C}$ be a path in the base of the fibration and let $\phi_t\colon Y_{\gamma(0)} \to Y_{\gamma(t)}$ be the symplectic parallel transport map. If $L \subset Y_{\gamma(0)}$ is a Lagrangian in the fibre then $\bigcup_{t\in[0,1]} \phi_t(L)$ is $\Omega$-Lagrangian $\mathcal{Y}$. Conversely, if $\mathcal{L} \subset \mathcal{Y}$ is a Lagrangian which lives submersively over $\gamma$ then $\mathcal{L} = \bigcup_{t\in[0,1]} \phi_t(\mathcal{L} \cap Y_{\gamma(0)})$.*

*Proof.* If $L \subset Y_{\gamma(0)}$ is Lagrangian and $\xi$ is a horizontal vector at $x$ then $\omega(T_xL, \xi) = 0$ because $\xi$ is symplectically orthogonal to fibres. If $\xi$ is the horizontal lift of $\dot\gamma$ then the submanifold $\bigcup_{t\in[0,1]} \phi_t(L)$ traced out by $L$ under parallel transport has tangent space $T_xL \oplus \langle\xi\rangle$, which is therefore Lagrangian.

Conversely, suppose $\mathcal{L} \subset \mathcal{Y}$ is a Lagrangian living submersively over $\gamma$. Let $x \in \mathcal{L}$ be a point with $\pi(x) = \gamma(t) =: s$ and let $\xi$ be a tangent vector to $\mathcal{L}$ whose projection $\pi_*\xi$ is $\dot\gamma(t)$. Let $\xi' \in \mathcal{H}_x$ be the horizontal lift of $\dot\gamma(t)$. Since $\pi_*\xi = \pi_*\xi'$, we have $\xi = \xi' + v$ for some vertical vector $v$. If we pick a symplectic basis[3] $e_1, \dots, e_{\dim Y_s}, f_1, \dots, f_{\dim Y_s}$ for $T_xY_s$ with $e_1, \dots, e_{\dim Y_s} \in T_x\mathcal{L}$ then there are numbers $\alpha_i, \beta_i$ such that

$$\xi = \xi' + \sum \alpha_i e_i + \sum \beta_i f_i.$$

Since $\mathcal{L}$ is Lagrangian, $\Omega(\xi, e_j) = 0$ for all $j$. Since $\xi'$ is horizontal, $\Omega(\xi', e_j) = 0$ for all $j$. Therefore $\beta_j = 0$ for all $j$, which means $\xi' = \xi - \sum \alpha_i e_i \in T_x\mathcal{L}$. That is, $\xi'$ is tangent to $\mathcal{L}$, which means that $\mathcal{L}$ is preserved by parallel transport. □

In our case, this means we can construct Lagrangians in $B_{d,p,q}$ just by taking a loop in a conic fibre and transporting it over a path in $\mathbf{C}$. The difficulty is in actually solving the parallel transport equation and seeing where a loop goes under parallel transport. Happily, there is a useful conserved quantity which solves this problem for us.

[3] i.e. $\Omega(e_i, f_j) = \delta_{ij}$.

**Lemma 1.18.** *The function* $H := \frac{1}{2}(|u|^2 - |v|^2)\colon B_{d,p,q} \to \mathbf{R}$ *is preserved by symplectic parallel transport in the conic fibration Equation* (1).

*Proof.* Recall that any function $H$ on a symplectic manifold defines a *Hamiltonian vector field* $V_H$ satisfying $\iota_{V_H}\omega = -dH$. The simplest example of this is if $\omega = dp \wedge dq$ on $\mathbf{R}^2$, in which case $V_H = (-\partial H/\partial q, \partial H/\partial p)$. In particular, if $H = \frac{1}{2}(p^2 - q^2)$ then $V_H = (-q, p)$, which generates a flow by rotations of $\mathbf{R}^2$. Therefore, the Hamiltonian $\frac{1}{2}(|u|^2 - |v|^2)$ generates the flow $(e^{i\theta}u, e^{-i\theta}v, w)$ on $B_{d,p,q}$. This flow preserves the fibres $uv = \text{const}$ so $V_H$ is vertical. If $\xi$ is a horizontal vector field then

$$\mathcal{L}_\xi H = dH(\xi)$$

but $dH(\xi) = -\omega(V_H, \xi)$. Since horizontal vectors are, by definition, symplectically orthogonal to vertical vectors, this means $dH(\xi) = 0$, so $H$ is preserved by parallel transport. □

For each conic fibre $\pi^{-1}(s)$, let $C_s$ be the circle $H^{-1}(0) \cap \pi^{-1}(s)$. Lemma 1.17 tells us that $V := \bigcap_{t\in[0,1]} C_{\gamma(t)}$ is a Lagrangian submanifold of $B_{d,p,q}$.

**Example 1.19.** If we look at the path $\gamma_k(t) = k + t$ for $k = 0, 1, 2, \ldots, d-1$ then:

- for $k = 1, 2, \ldots, d-1$ we get a Lagrangian sphere (the circles $C_{\gamma(t)}$ collapse to points as $t \to 0$ and $t \to 1$).
- for $k = 0$ we get a Lagrangian pinwheel. This is because the fibre over 0 is nonreduced, so the symplectic parallel transport map collapses $C_t$ $p$-to-1 onto $C_0$.

In the picture below, we draw this configuration $V$ in the case $d = 3$:

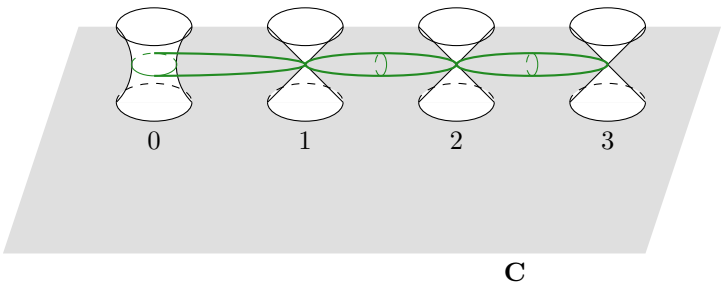


Finally, we show that this particular configuration $V$ is the vanishing cycle for the degeneration of $B_{d,p,q}$ to the T-singularity $\frac{1}{dp^2}(1, dpq - 1)$.

**Lemma 1.20.** *If we take the path* $\gamma(t) = 1 - t$ *in the base of the family* $X_s$ *then the vanishing cycle in* $X_1 = B_{d,p,q}$ *associated to the quotient singularity of* $X_0$ *is precisely* $V$.

*Proof.* Equip $\{(u,v,w,s) \in \mathbf{C}^4 \ : \ uv = (w^p - s)\cdots(w^p - ds)\}$ with the standard symplectic form coming from $\mathbf{C}^4$. Since the group $G'$ acts by symplectomorphisms on $\mathbf{C}^4$, this form descends to a symplectic form $\Omega$ on the total space $\mathcal{X} = \bigcup_{s\in\mathbf{C}} X_s$ of our degeneration.

By Lemma 1.17, we need to construct a Lagrangian submanifold $\mathcal{L}$ of $(\mathcal{X}, \Omega)$ such that $\mathcal{L} \cap X_1 = V$ and such that $\mathcal{L} \cap X_0$ contains $x_0$ (using the word submanifold in the loosest sense at this point).

Consider the antisymplectic involutions

$$\sigma_\pm \colon \mathbf{C}^4 \to \mathbf{C}^4, \qquad \sigma_\pm(u,v,w,s) = (\pm\bar{v}, \pm\bar{u}, \bar{w}, \bar{s}).$$

These preserve the equation $uv = (w^p - s)\cdots(w^p - ds)$, and commute with the action of $G'$, so descend to give antisymplectic involutions (which we continue to denote by $\sigma_\pm$ of $\mathcal{X}$.

The fixed locus of an antisymplectic involution is a Lagrangian submanifold, and $\mathcal{L} := \mathrm{Fix}(\sigma_-) \cup \mathrm{Fix}(\sigma_+)$ intersects $X_1$ in $\bigcup_{t\in\mathbf{R}} C_t$ (recall that $C_\star$ is the circle $H^{-1}(0) \cap \pi^{-1}(\star)$ where $\pi$ is the conic fibration $(u,v,w) \mapsto w^p$). From this it is easy to see that $V = \bigcup_{t\in[0,d]} C_t \subset X_1$ is the vanishing cycle, see the figure below. □

In this figure, we show a "movie" as $s$ varies over $[0,1]$ of the Lagrangians $\mathrm{Fix}(\sigma_-) \cap X_s$ (red) and $\mathrm{Fix}(\sigma_+) \cap X_s$ (green). In this case, $d = 3$. If $d$ were even then both of the noncompact pieces of the Lagrangian would be red.

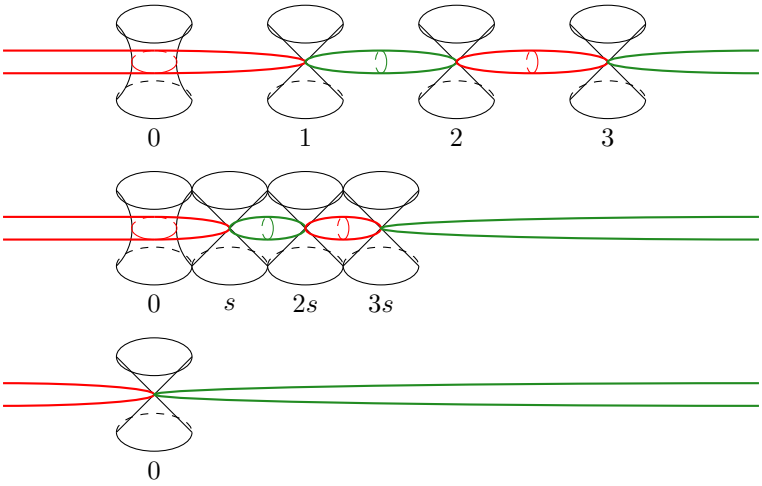

# 2 Lecture 2

In the previous lecture, we saw that the symplectic geometry of a smooth variety contains clues about the kinds of singularities that can form as the variety degenerates. We worked out in detail the example of cyclic quotient T-singularity $\frac{1}{dp^2}(1, dpq-1)$, identifying the link (a contact-type lens space $L(dp^2, dpq-1)$), the Milnor fibre (a codimension zero symplectic submanifold $B_{d,p,q}$) and the vanishing cycle (a chain of $d-1$ Lagrangian spheres attached to a Lagrangian pinwheel).

In this lecture, I want to explore the symplectic geometry of these manifolds $B_{d,p,q}$ more deeply and introduce a different way of representing them: the "almost toric pictures" discovered by Symington [17]. By the end of the lecture, we will be able to draw similar pictures of any smoothing of a cyclic quotient singularity. These almost toric pictures will be a key ingredient in Lecture 3.

## 2.1 Toric and almost toric pictures

To construct the family of $B_{p,q}$s, we will introduce a new way of representing $B_{d,p,q}$ called an *almost toric picture*. In this new representation, symplectically embedded $B_{d,p,q}$s are very visible. Almost toric pictures are generalisations of toric moment images, which we review first.

### 2.1.1 Toric varieties

Recall from Lemma 1.18 that a function $H$ on a symplectic manifold gives rise to a Hamiltonian vector field $V_H$ such that $\iota_{V_H}\omega = -dH$ and a Hamiltonian flow (the flow of $V_H$). If this flow is periodic with period $2\pi$ then we call the resulting circle action a *Hamiltonian circle action*.

If we have two Hamiltonian vector fields, associated to functions $H_1, H_2$ then the Lie bracket $[V_{H_1}, V_{H_2}]$ is again Hamiltonian, generated by the function $\{H_1, H_2\} = \omega(V_{H_1}, V_{H_2})$. This function is called *the Poisson bracket* of $H_1, H_2$. In particular, if the Poisson bracket vanishes then the flows commute (the converse is not true, e.g. consider the flows generated by the $x$ and $y$ coordinates on $\mathbf{R}^2$).

**Definition 2.1.** Suppose we have a collection of Hamiltonians $H_1, \ldots, H_n$ such that the Poisson brackets $\{H_i, H_j\}$ vanish and such that the lattice of periods

$$\Lambda = \{(t_1, \ldots, t_n) \in \mathbf{R}^n \ : \ \phi_{H_1}^{t_1} \cdots \phi_{H_n}^{t_n} = id\}$$

is $(2\pi\mathbf{Z})^n$. Then we get an action of the torus $\mathbf{R}^n/\Lambda$ which we call a *Hamiltonian torus action*.

*Remark* 2.2. If the Hamiltonian vector fields are linearly independent at some point $x$ then $n \leq \dim X/2$. To see this, note that the orbit through $x$ has tangent space spanned by the Hamiltonian vector fields, and $\omega$ vanishes on these vectors because the Poisson brackets are zero. Therefore the orbit is *isotropic* (the symplectic form vanishes on it) and an isotropic subspace can have dimension at most $\dim X/2$; if it has dimension $\dim X/2$ then it is called *Lagrangian*. If $n = \dim X/2$ then we say that $X$ is *toric*.

**Example 2.3.** Consider the Hamiltonians $H_1 = \frac{1}{2}|x|^2$, $H_2 = \frac{1}{2}|y|^2$ on $\mathbf{C}^2$. These Hamiltonians generate the Hamiltonian torus action $(x, y) \mapsto (e^{it_1}x, e^{it_2}y)$. The image of $\mathbf{C}^2$ by the map $\mu = (H_1, H_2)\colon \mathbf{C}^2 \to \mathbf{R}^2$ is the nonnegative quadrant in $\mathbf{R}^2$. The fibres of the map $\mu$ over the interior of this quadrant are Lagrangian tori. The fibres over the edges are circles and the fibre over the origin is a single point.

**Definition 2.4.** The map $\mu\colon X \to \mathbf{R}^n$ given by $\mu = (H_1, \ldots, H_n)$ is called the *moment map* and its regular fibres are Lagrangian tori. The image $\mu(X) \subset \mathbf{R}^n$ is a (possibly noncompact) convex polytope called the *moment image*. It is actually possible to reconstruct $X$ (up to equivariant symplectomorphism) from $\mu(X)$; this is Delzant's theorem [3, Theorem 2.1].

**Example 2.5.** The Hamiltonians $H_1, H_2$ from Example 2.3 descend to the quotient $\mathbf{C}^2/G$ where $G$ is the group of $n$th roots of unity acting by $(x, y) \mapsto (\mu x, \mu^a y)$. The quotient singularity $\frac{1}{n}(1, a)$ is therefore toric, however if we simply use $H_1, H_2$ as before then the period lattice is not standard: we have $\phi_{H_1}^{2\pi/n}\phi_{H_2}^{2\pi a/n} = id$. If instead we use the Hamiltonians

$$\left(H_2, \frac{1}{n}(H_1 + aH_2)\right)$$

then the lattice of periods becomes standard. The moment image is a convex wedge we will denote by $\pi(n, a)$:

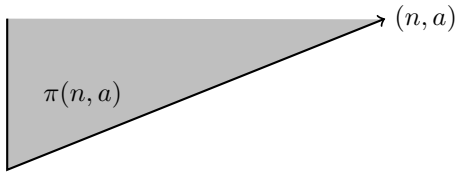


*Remark* 2.6. In this example, we made a $\mathbf{Q}$-affine change of Hamiltonians to change the period lattice. Note that $\mathbf{Z}$-affine changes of Hamiltonians leave the period lattice unchanged. In fact, if two toric manifolds have moment images which are related by a $\mathbf{Z}$-affine change of coordinates then they are equivariantly symplectomorphic.

*Remark* 2.7. In this example, we can see the contact lens space which is the link of the $\frac{1}{n}(1, a)$-singularity. It is simply the preimage of a horizontal line segment $\sigma$ running across $\pi(n, a)$. In 3-dimensional topology, lens spaces are defined to be

those orientable 3-manifolds containing a torus whose complement comprises two solid tori. In our toric picture, the preimage of the midpoint of $\sigma$ is a Lagrangian torus. The preimages of the left- and right-hand segments in $\sigma$ are solid tori, so we see that this is indeed a lens space (you have to work a little harder to see that it is $L(n, a)$).

### 2.1.2 Lagrangian torus fibrations

**Definition 2.8.** Let $X$ be a $2n$-dimensional symplectic manifold and $B$ be an $n$-dimensional stratified space. A Lagrangian torus fibration is a proper continuous map $F\colon X \to B$ such that:

- $F$ is a smooth submersion over the top stratum of $B$, with Lagrangian fibres;
- the fibres over other points are themselves stratified spaces, with isotropic strata.

*Remark* 2.9. The Arnold-Liouville theorem implies that the fibres over the top stratum are tori.

**Example 2.10.** If $X$ is toric then we can take $B$ to be the moment image and $F$ to be the moment map; this gives a Lagrangian torus fibration. The moment image is a convex polytope, so it is stratified by its faces. The top stratum is the interior: the fibres over this stratum are Lagrangian tori. Over points in faces of dimension $k$, the fibres are isotropic tori of dimension $k$.

**Example 2.11.** Consider

$$B_{d,p,q} = \{(u, v, w) \in \mathbf{C}^3 \ : \ uv = (w^p - 1) \cdots (w^p - d)\}/G'$$

and the holomorphic map $B_{d,p,q} \to \mathbf{C}$ given by $(u, v, w) \mapsto w^p$. Consider the functions $H_1 = \frac{1}{2}|w^p|^2$ and $H_2 = \frac{1}{2}(|u|^2 - |v|^2)$. The simultaneous level sets

$$H_1 = h_1, \quad H_2 = h_2$$

are tori whenever $h_1 \neq 0$ and $(h_1, h_2) \neq \left(\frac{1}{2}n^2, 0\right)$ for $n \in \{1, \ldots, d\}$. The fibres with $h_1 = 0$ are isotropic circles, and the fibres with $(h_1, h_2) = \left(\frac{1}{2}n^2, 0\right)$ are pinched tori. These pinched tori are stratified by isotropic strata: they are made up of a pinch point (0-stratum) and a Lagrangian cylinder (2-stratum).

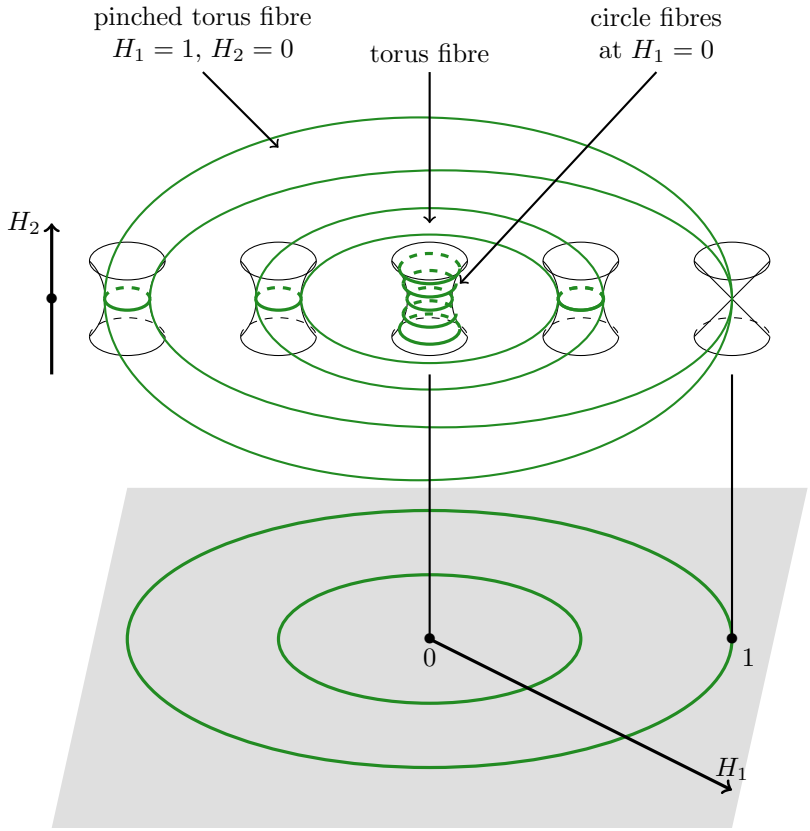


Here we draw (in the case $d = 3$) the image of the map $(H_1, H_2)\colon B_{d,p,q} \to \mathbf{R}^2$, denoting the pinched torus fibres with a cross:

(The picture should extend infinitely up, down and right.)

*Remark* 2.12.

1. The fibres over the vertical boundary are circles; the preimage of the vertical boundary is the conic at $H_1 = 0$. The local model for these kinds of singular fibre is precisely that of the boundary of the moment polygon in a toric surface.
2. The singularities in the pinched torus fibres are called "focus-focus singularities". Lagrangian torus fibrations with singularities modelled on focus-focus points and toric strata are called *almost toric fibrations*.
3. The precise horizontal position of the crosses is not really very important:

it can be changed by varying the equation for the smoothing.

4. The Lagrangian vanishing cycle we encountered last time is visible in this picture: it projects to the green line in the figure below.

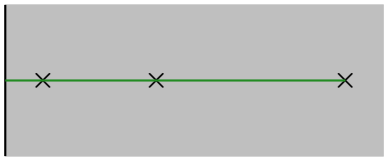

### 2.1.3 Action coordinates

This is not quite the end of the story. In toric geometry, we require that the period lattice be $(2\pi\mathbf{Z})^n$; without this condition, it is not possible to reconstruct the toric variety uniquely from the polytope. Indeed, as we saw in Example 2.5, if we don't impose this condition, then all the singularities $\frac{1}{n}(1,a)$ admit "moment maps" whose images are the nonnegative quadrant. In this case, we needed to correct our naive moment image by a $\mathbf{Q}$-affine transformation.

In our current example ($B_{d,p,q}$), the problem is even more severe: the Hamiltonian functions $H_1, H_2$ define an $\mathbf{R}^2$-action, but the flow of $H_1$ is not periodic: the focus-focus fibres each comprise two orbits of the $\mathbf{R}^2$-action, a fixed point (the node) and a Lagrangian cylinder, on which the flow of $H_1$ acts by translation (hence without periods). Even for the generic fibre, on which the flow of $H_1$ is periodic, its period varies from point to point.

We can fix this locally by using Hamiltonians of the form

$$(G(H_1, H_2), H_2).$$

Near a smooth torus fibre, it is always possible to find a $G$ such that these modified Hamiltonians generate a torus action with standard period lattice; the modified Hamiltonians are called *action coordinates*. This determines $G(H_1, H_2)$ uniquely up to adding on an integral multiple of $H_2$. It is usually nontrivial to find $G$ explicitly (even in simple Hamiltonian systems like the pendulum, its expression turns out to involve transcendental functions like elliptic integrals).

Globally, however, there are problems. For a start, $G$ will always be singular at the focus-focus fibres (there is no way to make a non-periodic flow periodic). Cut out these focus-focus fibres and fix our favourite smooth fibre. Solve for $G$ locally near that fibre, and prolong the solution to find $G$ everywhere away from the focus-focus fibres. If you prolong around a loop in the base which encloses some focus-focus fibres, then there is no guarantee that $G$ remains single-valued; the difference in values will be an integral multiple of $H_2$. In fact, a local computation shows that if you go once anticlockwise around a focus-focus fibre then the Hamiltonians $(G(H_1, H_2), H_2)$ become $(G(H_1, H_2) - H_2, H_2)$. In

other words, the *monodromy* for a focus-focus fibre is $M = \begin{pmatrix} 1 & -1 \\ 0 & 1 \end{pmatrix}$. See the example of monodromy for the spherical pendulum in [4] (he obtains the transpose-inverse of our monodromy, because he is interested in how monodromy acts on the homology of the torus fibres).

To combat this ambiguity, we will make branch cuts in the base of our torus fibration so as to remove the focus-focus fibres and ensure that the complement of the branch cuts is simply-connected. Then the action coordinates are well-defined on this domain. Without further justification, I will draw for you the result:

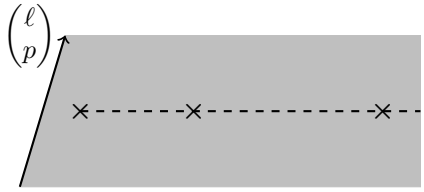


The slanted edge points in the direction $(\ell, p)$ where $\ell \in \{0, \ldots, p-1\}$ is the multiplicative inverse of $q$ mod $p$. The branch cuts are drawn as dotted lines. Changing coordinates using the $\mathbf{Z}$-affine transformation $N = \begin{pmatrix} p & -\ell \\ q & -k \end{pmatrix}$ (where $kp + q\ell = 1$) we get an alternative picture:

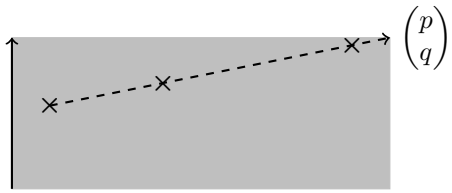


Here are some remarks:

- We have made our branch cuts in directions collinear with the eigenvector of the monodromy. If we had chosen another direction, our diagram would have been a sector with two dotted lines, related by the monodromy, and whenever you leave the sector by crossing one dotted line, you reappear at the other one with your tangent vector twisted by the monodromy matrix.
- In the latest picture, the monodromy matrix $M$ has changed to its conjugate $NMN^{-1} = \begin{pmatrix} 1+pq & -p^2 \\ q^2 & 1-pq \end{pmatrix}$ because we changed coordinates using $N$. It is easy to check that the branch cuts (now in direction $(p, q)$) are still pointing in the eigendirection of this matrix.

### 2.1.4 Mutation

One final modification will let us compare the toric picture of $\frac{1}{dp^2}(1, dpq-1)$ and the almost toric picture of its smoothing directly. We simply use a different set of branch cuts, pointing in the negative eigendirection. These branch cuts now intersect the toric boundary, which means that the vertical straight line in our earlier pictures appears bent in the new pictures. Nonetheless, it is still a straight line because when we cross the branch cut we must apply the monodromy to our tangent vectors. Because we are crossing $d$ branch cuts, each with monodromy $\begin{pmatrix} 1+pq & -p^2 \\ q^2 & 1-pq \end{pmatrix}$, the tangent vector $(0,-1)$ of our vertical line (travelling downwards) is sent to $(dp^2, dpq-1)$.

Here is the result; I will refer to this almost toric diagram as $\tilde{\pi}(dp^2, dpq-1)$.

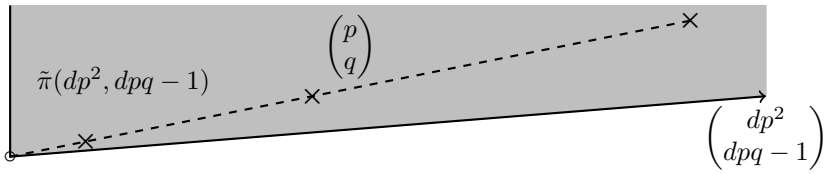


If we were to erase the branch cuts and decorations indicating the focus-focus fibres, we would obtain the standard moment polygon for the toric $\frac{1}{dp^2}(1, dpq-1)$ singularity.

*Remark* 2.13. This trick of changing branch cut by 180 degrees is called *mutation*. To perform a mutation, we slice our picture in two using the branch cut, we apply the monodromy to one of the two halves and then reattach them. This will be an important operation in what follows. Note that mutation does not change the symplectic manifold or even the torus fibration, it only changes the choice of branch cut used in producing the action coordinates.

## 2.2 Smoothings of other cyclic quotient singularities

We can now draw almost toric pictures for smoothings of other cyclic quotient singularities.

### 2.2.1 Kollár–Shepherd-Barron classifications

The **Q**-Gorenstein smoothings of cyclic quotient singularities were classified by Kollár and Shepherd-Barron [11]. Here was their idea:

- Take a **Q**-Gorenstein smoothing $\mathcal{X} \to \mathbf{C}$ where $X_0 = \mathbf{C}^2/G$ is the singularity of type $\frac{1}{n}(1, a)$. Write $x_0 \in X_0$ for the singular point.

- The total space $\mathcal{X}$ is usually singular at $x_0$. By the semistable reduction theorem, you can perform base-change and birationally modify $\mathcal{X}$ to get a new smoothing $\mathcal{X}' \to \mathbf{C}$ with smooth total space, and to make $X_0'$ into a reduced simple normal crossing divisor.
- Using the semistable minimal model program, you can further modify $\mathcal{X}$ to get a smoothing $\mathcal{X}'' \to \mathbf{C}$ so that any curve $C$ contracted by the birational map $\mathcal{X}'' \to \mathcal{X}$ satisfies $K_{\mathcal{X}''} \cdot C > 0$. The cost of this step is that you may introduce terminal singularities in the total space.
- The cyclic quotient singularities whose $\mathbf{Q}$-Gorenstein smoothings have at worst isolated terminal singularities are classified by Kollár and Shepherd-Barron; they are precisely the T-singularities we have already discussed.

Therefore, after all of this messing around, we have a central fibre $X_0''$ which is a partial resolution of the original $X_0$, obtained by blowing up some sequence of points. The singularities of $X_0''$ are T-singularities and the canonical class evaluates nonnegatively on curves. We finally take the canonical model; this may introduce some ADE singularities, but ensures that the canonical class evaluates positively on all curves.

**Definition 2.14** (P-resolution)**.** A partial resolution $f\colon Y_0 \to X_0$ of a cyclic quotient singularity is called a *P-resolution* if:

- it has only T-singularities,
- $K_{Y_0}$ evaluates positively on all exceptional curves of $f$.

### 2.2.2 Toric P-resolutions and their almost toric smoothings

In terms of toric pictures, partial resolution is accomplished by making truncations to the moment polygon (just as blowing up a smooth toric fixed point amounts to chopping off a corner of the moment polytope). It turns out that there are only a finite number of truncations giving a P-resolution (for an explanation of this, and how to find the P-resolutions, see [11, Section 3]; I have given a brief, pragmatic account in Appendix A).

**Example 2.15** ([11, Example 3.15])**.** There are three P-resolutions of the singularity $\frac{1}{19}(1,7)$. In each case, we draw the toric model and indicate the singular points as red dots. I have also written the type of the singularity (not to be confused with the slope-vectors labelling the edges).

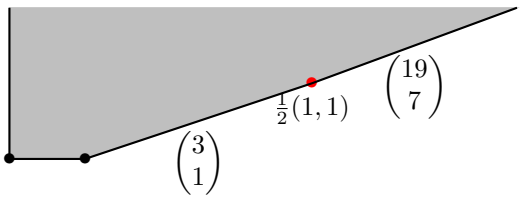

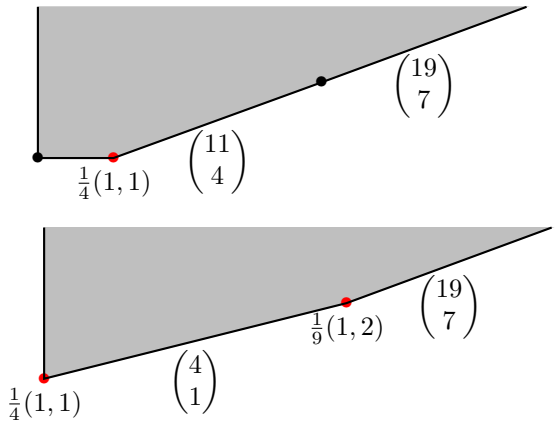


Each singular point is a T-singularity and can be smoothed by implanting the local almost toric model at the relevant vertex. We must be careful to use a $\mathbf{Z}$-affine transformation to transfer the almost toric diagram $\tilde{\pi}(dp^2, dpq-1)$ to the relevant vertex.

In the first picture, for example, we use $A = \begin{pmatrix}11 & -3\\ 4 & -1\end{pmatrix}$ to put the vector $(0,1)$ into the $(-3,-1)$-direction and $(2,1)$ into the $(19,7)$-direction. The branch cuts now must point in the $A\begin{pmatrix}1\\1\end{pmatrix} = \begin{pmatrix}8\\3\end{pmatrix}$-direction. Here are the resulting diagrams (not all are drawn to scale because some branch cuts are almost parallel to the boundary):

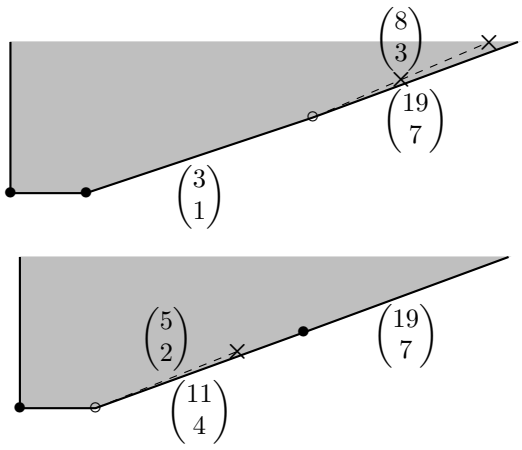

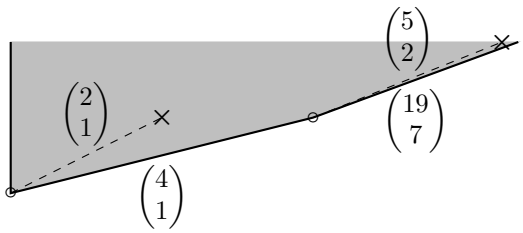


(I've drawn the smoothed vertices as open circles, to distinguish them from the actual vertices: remember that the 'broken edge' passing through a smoothed vertex is really a straight line). In particular, we see that:

- the first example contains a symplectically embedded $B_{2,1,1}$ (neighbourhood of a Lagrangian sphere),
- the second example contains a symplectically embedded $B_{2,1}$ (neighbourhood of a Lagrangian $(2,1)$-pinwheel, i.e. $\mathbf{RP}^2$.
- the third example contains a symplectically embedded $B_{2,1}$ and a symplectically embedded $B_{3,1}$ (neighbourhood of a Lagrangian $\mathbf{RP}^2$ and a $(3,1)$-pinwheel).

These manifest themselves in our almost toric pictures as preimages under the torus fibration of neighbourhoods of the dashed lines.

*Remark* 2.16. Consider the lens space $L(n,a)$ equipped with the contact structure it inherits as the link of $\frac{1}{n}(1,a)$. The minimal symplectic fillings of this contact manifold were classified up to diffeomorphism by Lisca [12]. It was proved in [14] that his classification coincides with that of Kollár–Shepherd-Barron; that is any minimal symplectic filling is diffeomorphic to a smoothing of the corresponding cyclic quotient singularity and smoothings coming from different P-resolutions are not diffeomorphic (it seems likely that this classification holds up to the stronger equivalence relation given by symplectic deformation/diffeomorphism, but I believe this statement is still open).

# 3 Lecture 3

## 3.1 Applications

Next, I want to review some of the theorems you can prove using symplectic techniques to put constraints on singularity formation.

**Theorem 3.1** (Evans-Smith [6]). *Suppose that we have $N$ disjointly and symplectically embedded submanifolds $U_1, \dots, U_N \subset \mathbf{CP}^2$ where each $U_i$ is a copy of $B_{p_i,q_i}$. Then $N \leq 3$ and $\{p_1, p_2, \dots, p_N\}$ is a subset of a Markov triple, that is a solution $\{a, b, c\}$ to the Diophantine equation $a^2 + b^2 + c^2 = 3abc$ (moreover, the $q$s are determined by the $p$s in the triple).*

Note that $d = 1$ for any $B_{d,p,q} \subset \mathbf{CP}^2$ because $\mathbf{CP}^2$ contains no Lagrangian spheres (just for homology reasons).

*Remark* 3.2. This theorem is a symplectic geometer's translation of the following, earlier theorem of Hacking and Prokhorov, which inspired it:

**Theorem 3.3** (Hacking-Prokhorov [8, 9]). *Suppose $\mathcal{X} \to S$ is a $\mathbf{Q}$-Gorenstein degeneration whose general fibre is $\mathbf{CP}^2$ and whose singular fibre $X_0$ has ample anticanonical bundle and at worst isolated quotient singularities. Then $X_0$ is a ($\mathbf{Q}$-Gorenstein deformation of) a weighted projective space $P(p_1^2, p_2^2, p_3^2)$ where $\{p_1, p_2, p_3\}$ is a Markov triple. (These weighted projective spaces have precisely three singularities of type $\frac{1}{p_i^2}(1, p_i q_i - 1)$).*

**Theorem 3.4** (Evans-Smith [5]). *Let $X$ be a smooth surface of general type with $p_g > 0$ ($b^+ > 1$) equipped with its canonical symplectic form and suppose it contains a symplectically embedded copy of $B_{p,q}$ for some $p, q$. Let $\ell$ be the length of the continued fraction expansion*

$$\frac{p^2}{pq - 1} = b_1 - \frac{1}{b_2 - \frac{1}{\dots - \frac{1}{b_\ell}}}.$$

*Then $\ell \leq 4K^2 + 7$.*

*Remark* 3.5. The canonical symplectic form is obtained as follows. The canonical bundle of $X$ is nef and big, and vanishes only along a collection of embedded rational$-2$-curves. The (pluri)canonical map contracts these $-2$-curves, so the canonical model is a surface with ADE singularities. We can now perform symplectic surgery, cutting out these singularities and replacing them with copies of the ADE Milnor fibres. The result is a smooth symplectic manifold whose symplectic form is *negatively monotone*, i.e. it satisfies $[\omega] = K_X$.

*Remark* 3.6. This theorem implies the corresponding bound for lengths of singularities in stable degenerations of general type surfaces (in a stable degeneration, the central fibre has ample canonical bundle, which means that the canonical symplectic form makes sense over the whole family, allowing us to define symplectic parallel transport). This bound (in fact, a slightly better bound

of $\ell \leq 4K^2 + 1$) was proved independently and simultaneously using purely algebro-geometric techniques in a paper by Rana and Urzúa [16].

In this lectures, I will not discuss these theorems any further, because the proofs require techniques of pseudoholomorphic curve theory and Seiberg-Witten theory which I would not have time to cover. Instead, I will try to explain the proof of the following theorem, and what it has to do with algebraic geometry (specifically the minimal model program).

**Theorem 3.7** (Evans-Urzúa [7])**.** *Let $X$ be the quintic surface. There exists a symplectic form $\omega$ on $X$ which is a deformation of its canonical symplectic form and such that $(X, \omega)$ contains symplectically embedded copies of $B_{p_i,q_i}$ for $p_i, q_i$ on the following list:*

$$(5, 3),\ (14, 9),\ (37, 24),\ \ldots$$

*This is an infinite list, where $p_i$ and $q_i$ both satisfy the recursion relation*

$$\begin{pmatrix} 0 & 1 \\ -1 & \delta \end{pmatrix} \begin{pmatrix} p_i \\ p_{i+1} \end{pmatrix} = \begin{pmatrix} p_{i+1} \\ p_{i+2} \end{pmatrix}, \qquad \delta = p_i q_{i+1} - p_{i+1} q_i = 3.$$

The reason we are allowed to violate the inequality $\ell \leq 4K^2 + 7$ is because the symplectic form is not the canonical one. It would be interesting to investigate in greater detail how the symplectic embeddability of $B_{p,q}$s depends on the cohomology class of $\omega$.

*Remark* 3.8. Though this theorem is about quintic surfaces, we have other examples, and indeed we expect that such sequences of symplectic embeddings of unbounded length can be constructed in symplectic deformations of most general type surfaces.

*Remark* 3.9. The proof of Theorem 3.7 draws heavily on ideas from the paper [10] of Hacking, Tevelev and Urzúa. Indeed, our paper [7] can be seen as a symplectic account of what is happening in [10].

We will start our proof of Theorem 3.7 with an example.

## 3.2 An example: the $\frac{1}{11}(1, 3)$ singularity

Consider the cyclic quotient singularity $\frac{1}{11}(1, 3)$.

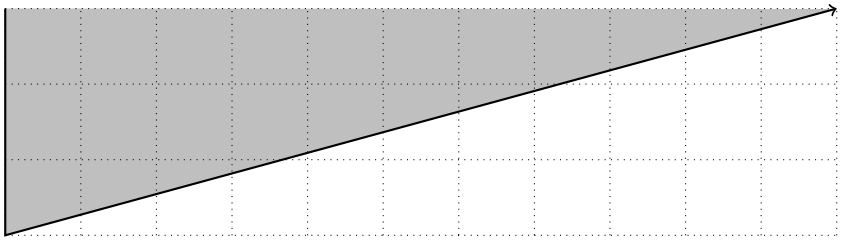

We will truncate this polygon with a line pointing in the $(1,-2)$-direction. Let us call the resulting polygon $\Pi^-$:

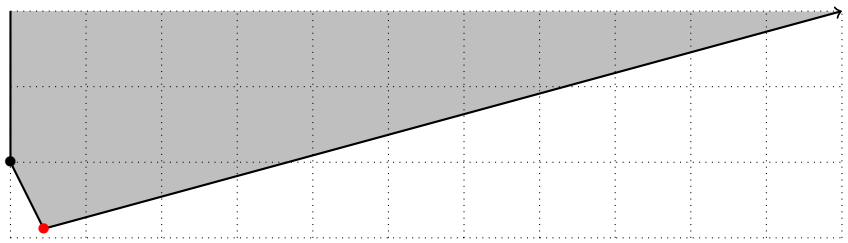

The associated toric variety $V_{\Pi^-}$ is **not** a P-resolution of $\frac{1}{11}(1,3)$: if you evaluate the canonical class on the curve which lives over the line we introduced by truncation then you get a negative number (see Appendix A). Nonetheless, we can check that $V_{\Pi^-}$ has only T-singularities:

- the left-hand vertex is actually a smooth point: the outgoing edges point in the directions $(0,1)$ and $(1,-2)$, which form an integral basis for the lattice $\mathbf{Z}^2$.
- the right-hand (red) vertex is a $\frac{1}{25}(1,14)$-singularity, whose smoothing will be a $B_{5,3}$. To see this, note that the matrix $\begin{pmatrix} 1 & -1 \\ -1 & 2 \end{pmatrix}$ sends $(0,1)$ and $(25,14)$ (the outgoing edges in the standard polygon $\tilde{\pi}(25,14)$) to $(-1,2)$ and $(11,3)$ respectively, which are the outgoing edges at this vertex. The branch cut points in the direction

$$\begin{pmatrix} 1 & -1 \\ -1 & 2 \end{pmatrix} \begin{pmatrix} 5 \\ 3 \end{pmatrix} = \begin{pmatrix} 2 \\ 1 \end{pmatrix}.$$

Let us write $U_{\Pi^-}$ for the smoothing of $V_{\Pi^-}$. From what we just said, $U_{\Pi^-}$ has the following almost toric picture, in which we can see a symplectically embedded $B_{5,3}$ living over the blue-shaded region:

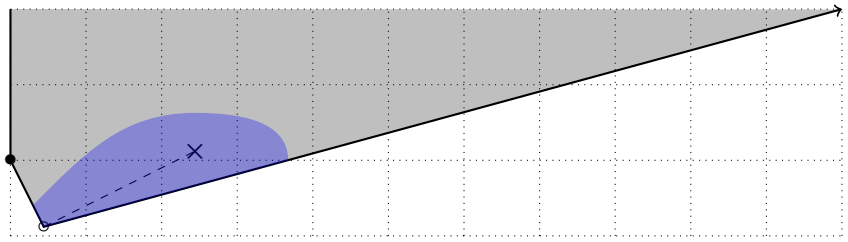

By Lisca's classification, this must be diffeomorphic to one of the smoothings which comes from a P-resolution, but how can we identify which one?

First, let us perform a mutation and rotate the branch cut anticlockwise by 180 degrees; we know that the broken edge which used to meet the branch cut will

become a straight line after this mutation, so we don't need to think about it too much.

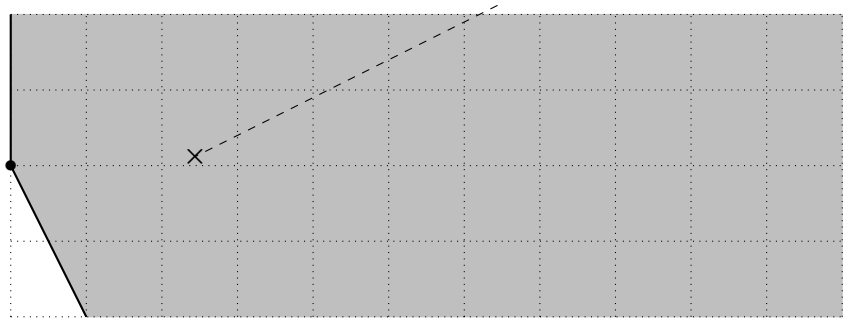

Now I want to change the picture by moving the focus-focus singularity and the branch cut in parallel to the north-west.

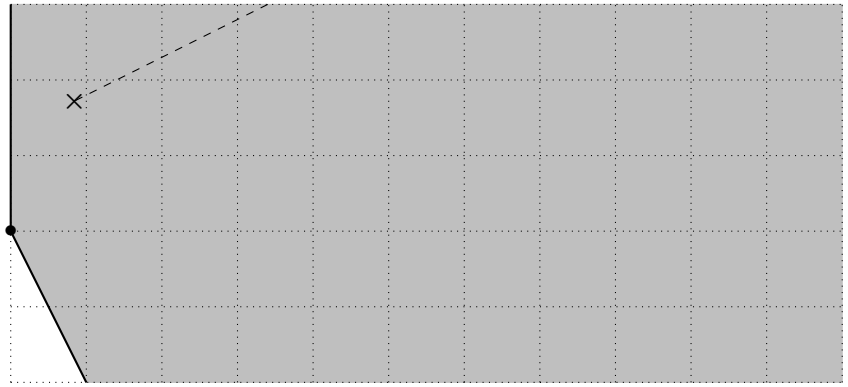

Finally, we mutate back, rotating the branch cut 180 degrees clockwise. We need to think about this: the monodromy for the branch cut in $\tilde{\pi}(25,14)$ is $M = \begin{pmatrix} 16 & -25 \\ 9 & -14 \end{pmatrix}$; we used $N = \begin{pmatrix} 1 & -1 \\ -1 & 2 \end{pmatrix}$ to put $\tilde{\pi}(25,14)$ into position at the vertex in our picture, so the monodromy matrix becomes $NMN^{-1} = \begin{pmatrix} 3 & -4 \\ 1 & -1 \end{pmatrix}$. Applying this to the red shaded region in the picture, we need to see where the vectors $(0,-1)$ and $(1,-2)$ end up (as these are the slopes of the edges in this region).

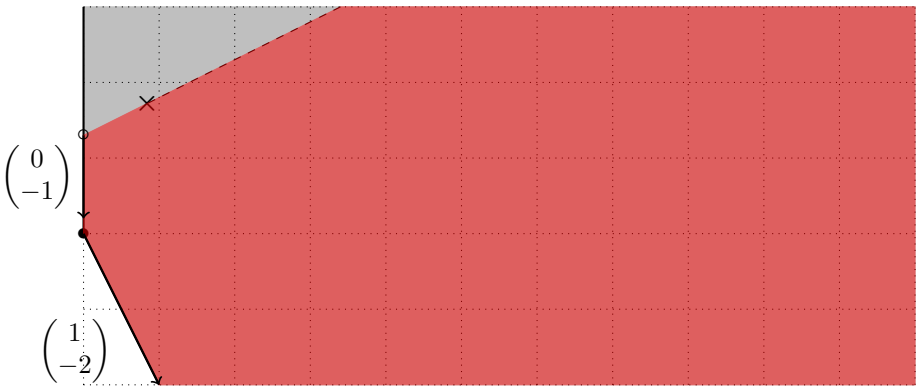


They go to $(4, 1)$ and $(11, 3)$, so we end up with the diagram below (not drawn to scale: $(4, 1)$ and $(11, 3)$ are very close to parallel).

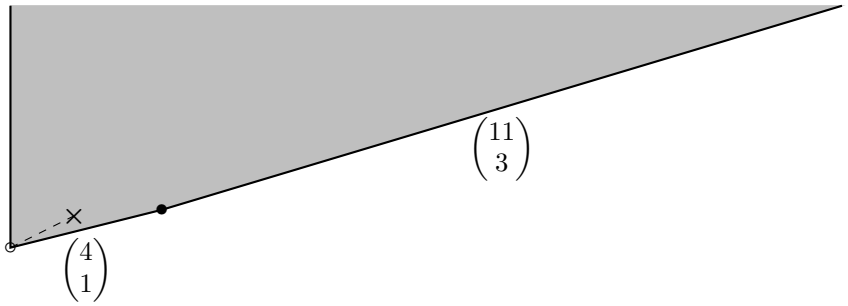


Let us call the resulting polygon $\Pi^+$, the corresponding toric variety $V_{\Pi^+}$ and the almost toric manifold determined by the picture above $U_{\Pi^+}$ (so $U_{\Pi^+}$ is a smoothing of $V_{\Pi^+}$). The variety $V_{\Pi^+}$ is a P-resolution of $\frac{1}{11}(1, 3)$, which tells us whereabouts in the Kollár–Shepherd-Barron/Lisca classification the smooth 4-manifold $U_{\Pi^-}$ lives.

*Remark* 3.10. How do you know if a given toric diagram defines a P-resolution? Once you've checked that the vertices are locally isomorphic to wedges of the form $\pi(dp^2, dpq - 1)$, you still need to check that the canonical class evaluates positively on the rational curves which make up the compact part of the toric divisor. I endeavour to explain how to check this in an appendix to these notes.

## 3.3 Moving the singularity

In the previous example, we performed an operation which we have not yet justified. Namely, we deformed the almost toric picture by moving the focus-focus singularity and its branch cut in parallel to the north-west.

We have already mentioned (Remark 2.12(3), see also [17, Proposition 6.2]) that you can move the focus-focus singularity in the direction which is an eigenvector

for its monodromy (i.e. along its branch cut, if you have chosen your branch cut to point along this eigenvector); this changes the Lagrangian torus fibration, but it does not change the total space up to symplectomorphism. In the language of Symington [17], this is a *nodal slide*.

However, if we wish to move the focus-focus singularity in a different direction, we will need to deform the symplectic form in a more serious way. Any almost toric picture with contractible base[4] specifies for us a symplectic manifold [17, Corollary 5.4] unique up to symplectomorphism. This works in much the same way that it does in the toric setting, except that we need to be slightly careful about how to handle the focus-focus singularities. The resulting manifold is only determined up to symplectomorphisms which do not necessarily preserve the Lagrangian torus fibrations (while a toric moment image determines the manifold up to equivariant symplectomorphisms, which preserve the torus fibrations).

Our one-parameter family of almost toric pictures gives us a one-parameter family $\omega_t$ of symplectic structures, but $\omega_0$ and $\omega_1$ will not be symplectomorphic:

**Lemma 3.11.** *In a family $\omega_t$ of symplectic forms on $U_{\Pi^-}$ determined by the above sequence of almost toric pictures, $[\omega_0]$ is a negative multiple of the canonical class $K$ and $[\omega_1]$ is a positive multiple of $K$.*

*Proof.* Note that $H_2(U_{\Pi^-}; \mathbf{Z}) = \mathbf{Z}$; we can see a generator as follows. Consider the almost toric picture at the beginning of the sequence:

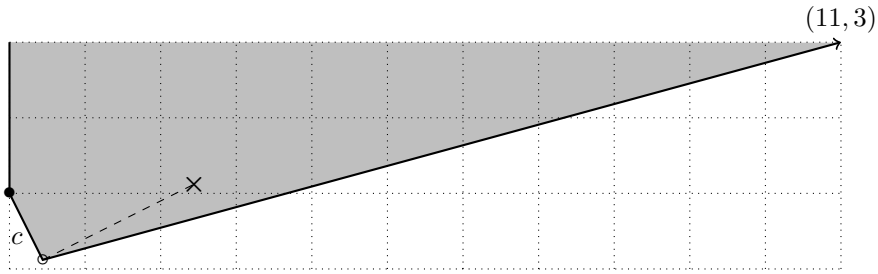


Consider the following chains:

- $C$: the preimage of the edge $c$ in the almost toric picture
- $L$: the Lagrangian pinwheel living over the branch cut.

These are both discs with a common boundary (the circular fibre over the vertex marked with a circle), however, the pinwheel wraps $p = 5$ times around this circle, so to get a closed cycle we must take $G_{\Pi^-} = 5C - L$. This cycle $G_{\Pi^-}$ generates $H_2(U_{\Pi^-}; \mathbf{Z})$. We have $\int_{G_{\Pi^-}} \omega_0 > 0$ because $C$ has positive symplectic

[4] If the base has nontrivial topology then there is an additional *Lagrangian Chern class* which can distinguish between fibrations over this base, [18].

area and $L$ has zero symplectic area. Moreover, it is possible to check that $K \cdot G_{\Pi^-} < 0$ (this is equivalent to saying that $V_{\Pi^-}$ is not a P-resolution of $\frac{1}{11}(1,3)$).

If we do the same construction for the almost toric picture at the end of the sequence:

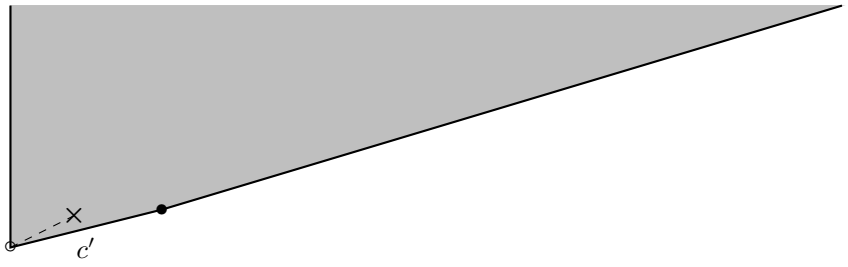


then we get a cycle $G_{\Pi^+}$ with $\int_{G_{\Pi^+}} \omega_1 > 0$, but now $K \cdot G_{\Pi^+} > 0$.

Since $H^2(U_{\Pi^-}; \mathbf{R}) = \mathbf{R}$, the symplectic form falls into one of the following classes:

- positively monotone (if its integral over some cycle $D$ is positive but $K \cdot D < 0$)
- negatively monotone (if its integral over some cycle $D$ is positive and $K \cdot D > 0$)
- exact (if its integral over any cycle is zero).

Clearly $\omega_0$ is positively monotone, $\omega_1$ is negatively monotone (and, for some $t \in (0,1)$, $\omega_t$ is exact). □

*Remark* 3.12. If we revisit the proof of the Kollár–Shepherd-Barron classification, we see that there is a magical step where you apply the semistable minimal model program to the total space of your smoothing. In the current context, this means that you apply Mori flips to replace $K$-negative curves by $K$-positive curves. Before the flip, in fact, $-K$ is ample on the central fibre and hence (by openness of amplitude) relatively ample on some neighbourhood of the central fibre, so we get an anticanonical (positively monotone) symplectic form on nearby fibres. After the flip, $K$ is relatively ample, and we get a canonical (negatively monotone) symplectic form on every fibre. Our construction interpolates between these two symplectic forms. The fact that the surfaces before and after the flip really coincide with the toric surfaces $V_{\Pi^-}$ and $V_{\Pi^+}$ follows from the paper [10].

## 3.4 Infinitely many mutations

### 3.4.1 Nodal trades

The construction of a Lagrangian torus fibration on the smoothing of the $\frac{1}{dp^2}(1, dpq-1)$ singularity works just as well when we have a smooth point (e.g. $d = p = 1$, $q = 0$) and gives us the following almost toric picture of the ball:

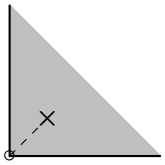

I like to call this Hamiltonian system the *Auroux system* because I learned of it from Auroux's classic paper on Fano mirror symmetry [1].

In a toric moment polygon, a corner corresponds to a smooth point of the toric variety if it has a neighbourhood which is $\mathbf{Z}$-affine isomorphic to the nonnegative quadrant in $\mathbf{R}^2$. We can therefore replace such a local Lagrangian torus fibration with the Auroux system. Symington calls this operation a *nodal trade* and shows [17, Theorem 6.5] that it doesn't change the symplectomorphism type of the manifold, only the Lagrangian torus fibration.

### 3.4.2 Back to $\frac{1}{11}(1, 3)$

Let us return to our example $U_{\Pi^-}$:

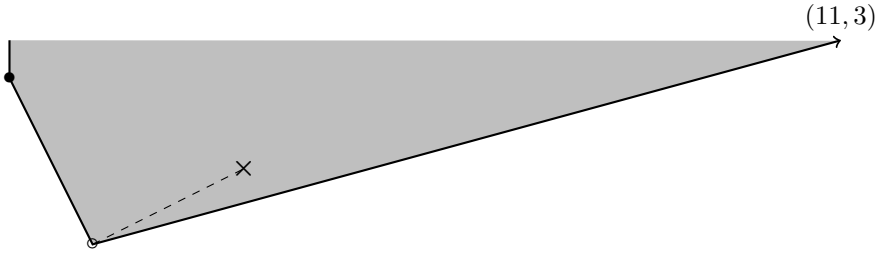


We may perform a nodal trade at the remaining vertex to obtain the following almost toric picture:

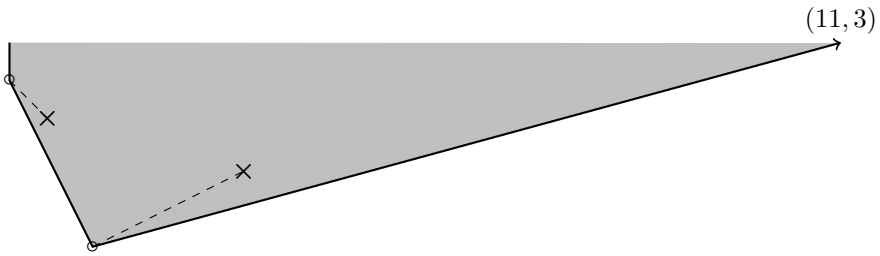


Let us perform a nodal slide to make the right-hand branch cut very small:

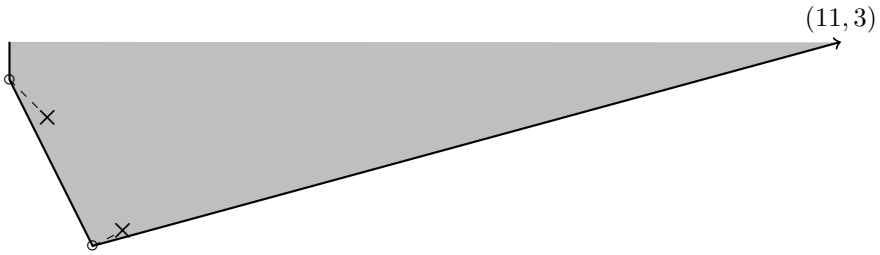


and mutate by rotating the left-hand branch cut anticlockwise 180 degrees; this means applying a matrix $M$ to the lower half of the diagram and we can figure out $M$ as follows:

- we know that the vertices marked with circles are not really breaking points and the edge passing through that point is a straight line, so we need $M \begin{pmatrix} 1 \\ -2 \end{pmatrix} = \begin{pmatrix} 0 \\ -1 \end{pmatrix}$.
- we know that the vector $(1, -1)$ is a 1-eigenvector of $M$.

The only possibility is $M = \begin{pmatrix} 2 & 1 \\ -1 & 0 \end{pmatrix}$, and we see that the edge pointing in the $(11, 3)$-direction will end up pointing in the $(25, -11)$-direction:

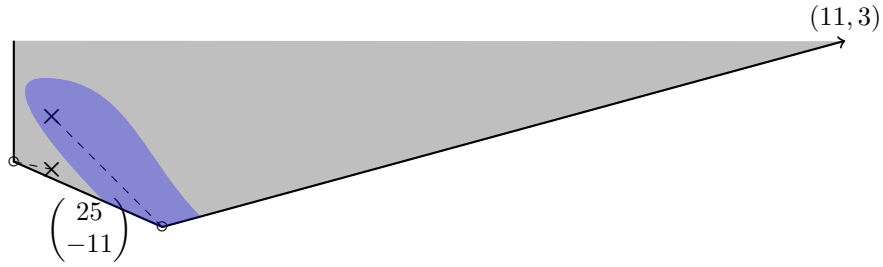


(and the other branch cut, which formerly pointed in the $(2, 1)$-direction now points in the $(5, -2)$-direction.

**Lemma 3.13.** *The preimage of the blue region in this picture is a copy of* $B_{14,9}$.

*Proof.* The matrix $\begin{pmatrix} 11 & 25 \\ 7 & 16 \end{pmatrix}$ sends $(-25, 11)$ and $(11, 3)$ to $(0, 1)$ and $(196, 125)$ respectively, so this vertex is locally modelled on $\tilde{\pi}(196, 125)$. Note that $196 = 14^2$ and $125 = 14 \times 9 - 1$ so this is the almost toric model for $B_{14,9}$. □

After making another nodal slide to put this branch cut out of the way, we can now mutate at the other branch cut and we obtain a copy of $B_{37,24}$. Continuing in this manner, we get a whole sequence of symplectically embedded rational homology balls.

*Remark* 3.14. It is a slightly fiddly exercise in affine geometry to check that the $p_i, q_i$ we obtain in this manner satisfy the recursion formula stated in Theorem 3.7; a sequence $p_i, q_i$ satisfying this recursion is called a *Mori sequence*.

**Lemma 3.15.** *If $X$ is a compact symplectic 4-manifold which admits a symplectic embedding of $U_{\Pi^+}$ then some symplectic deformation of $X$ admits a symplectic embedding of infinitely many rational homology balls $B_{p_i,q_i}$ for a Mori sequence $(p_i, q_i)$.*

*Proof.* Let us be slightly more precise about the size of neighbourhoods. Let $\Pi^-(a, h)$ denote the bounded polygon obtained by rescaling $\Pi^-$ until the compact edge $c$ (with slope $-2$) has affine length $a$ and truncating[5] from above at height $h$. We have seen that you can deform the symplectic form on $U_{\Pi^+}$ to get $U_{\Pi^-}(a, h)$ for some $a, h$. By a further deformation, we can make $a$ arbitrarily small (this amounts to moving the truncating edge $c$ closer to the origin, and is known in symplectic geometry as *symplectic deflation*). It is another fiddly exercise in affine geometry [7, Lemma 3.13] to show that you can do arbitrarily many mutations to $\Pi^-(a, h)$ if $a \ll h$. Therefore $U_{\Pi^-(a,h)}$, the part of $U_{\Pi^-}$ living over $\Pi^-(a, h))$ contains a Mori sequence of rational homology balls, which we now find in this deformation of $X$. □

We now apply this result to the quintic surface.

## 3.5 The quintic surface

Consider the surface $\mathbf{CP}^1 \times \mathbf{CP}^1$ and let $B$ be a curve of bidegree $(6, 6)$ which:

- intersects the diagonal $\mathbf{CP}^1$ at six points each with multiplicity 2,
- intersects some fixed ruling $\mathbf{CP}^1 \times \{z\}$ at three points each with multiplicity 2.

Take a double cover of $\mathbf{CP}^1 \times \mathbf{CP}^1$ branched along $B$. The preimage of the diagonal is then a pair of rational $-4$-curves (intersecting at six points) and the preimage of the ruling is a pair of rational $-3$-curves (intersecting at three

[5] Here we just mean to excise everything above height $h$ from the manifold, not to make a symplectic cut at that height.

points). If we pick one of these $-4$-curves $C_1$ and one of these $-3$-curves $C_2$ then they intersect at a single point (just like the diagonal and the ruling).

Let us collapse the curves $C_1, C_2$. We obtain a singularity of type $\frac{1}{11}(1,3)$: collapsing a chain of rational curves $C_1, \dots, C_\ell$ with self-intersections $-b_1, \dots, -b_\ell$ like this yields the cyclic quotient singularity $b_1 - \frac{1}{b_2 - \frac{1}{\cdots - \frac{1}{b_\ell}}}$, and $\frac{11}{3} = 4 - \frac{1}{3}$.

This singular surface $Z$ has a P-resolution $Y \to Z$; $Y$ is obtained from the branched double cover by collapsing $C_1$. This is the P-resolution we have been studying (corresponding to the polygon $\Pi^+$). The surface $Y$ is a stable quintic surface with a $\frac{1}{4}(1,1)$-singularity. By a theorem of Rana [15, Theorem 4.10], this quintic is smoothable and, by construction, this smoothing contains a symplectically embedded $U_{\Pi^+}$ (symplectic with respect to the (negatively monotone) canonical symplectic form). By Lemma 3.15, we can make a deformation of the symplectic form on the quintic, supported on $U_{\Pi^+}$, so that the new symplectic form admits symplectic embeddings of $B_{p_i,q_i}$ for a Mori sequence $p_i, q_i$, which proves Theorem 3.7.

# A Appendix: P-resolutions

In this appendix, I explain how you can tell if a partial resolution of a cyclic quotient singularity is a P-resolution or not. The appendix is a modification of a blog post I wrote on 4th June 2018 (http://jde27.uk/blog/cyclic2.html).

## A.1 Discrepancies

Let $X$ be a cyclic quotient singularity of type $\frac{1}{n}(1,a)$ and let $\pi\colon \tilde{X} \to X$ be its minimal resolution. The exceptional locus of $\pi$ comprises a chain of rational curves $C_1, \dots, C_\ell$ with $C_i^2 = -b_i$ where

$$\frac{n}{a} = b_1 - \frac{1}{b_2 - \frac{1}{\cdots - \frac{1}{b_\ell}}}.$$

(See my earlier blog post http://jde27.uk/blog/cyclic1.html for an explanation of this in terms of truncations of the moment polygon). Our first goal is to express the canonical class $K_{\tilde{X}} = -c_1(\tilde{X}) \in H^2(\tilde{X}; \mathbf{Z})$ in terms of Poincaré-duals of the closed curves $C_1, \dots, C_\ell$ in $\tilde{X}$. However, $\tilde{X}$ is not compact, so we must make do with Alexander-Lefschetz duality $H^2(\tilde{X}; \mathbf{Z}) \cong H_2(\tilde{X}, \partial\tilde{X}; \mathbf{Z})$. The compact curves $C_1, \dots, C_\ell$ do not generate $H_2(\tilde{X}, \partial\tilde{X}; \mathbf{Z})$, rather they span the image of the map $H_2(\tilde{X}; \mathbf{Z}) \to H_2(\tilde{X}, \partial\tilde{X}; \mathbf{Z})$, whose cokernel is the finite group $H_1(\partial\tilde{X}; \mathbf{Z}) = \mathbf{Z}/n$ by the long exact sequence of the pair $(\tilde{X}, \partial\tilde{X})$. If we work over $\mathbf{Q}$ then this cokernel vanishes, but we are then forced to write $K_{\tilde{X}}$ as a *rational* linear combination of the Alexander-Lefschetz duals of $C_1, \dots, C_\ell$:

$$K_{\tilde{X}} = \sum k_i C_i.$$

The numbers $k_i$ are called the *discrepancies* of the singularity (they measure the discrepancy between $K_{\tilde{X}}$ and $\pi^* K_X = 0$).

We have the adjunction formula $K_{\tilde{X}} \cdot C_i = -C_i^2 - 2$ for each $i$. Substituting $K_{\tilde{X}} = \sum k_i C_i$, we obtain a system of simultaneous equations

$$\sum k_i E_i \cdot E_j = b_j - 2, \quad j = 1, \ldots, \ell,$$

for the discrepancies.

**Example A.1.** Consider the minimal resolution of the $\frac{1}{4}(1,1)$ singularity which has exceptional locus $C_1$ with $C_1^2 = -4$. Then we have $-4k_1 = 2$ so $k_1 = -1/2$.

**Example A.2.** Consider the minimal resolution of the $\frac{1}{11}(1,3)$ singularity which has exceptional locus $C_1 \cup C_2$ with $C_1^2 = -4$, $C_2^2 = -3$ and $C_1 \cdot C_2 = 1$. Then we have

$$-4k_1 + k_2 = 2, \qquad k_1 - 3k_2 = 1,$$

or $k_1 = -7/11$, $k_2 = -6/11$.

*Remark* A.3. A singularity is called *terminal* if all the discrepancies are positive, *canonical* if they are nonnegative, *log terminal* if they are $> -1$ and *log canonical* if they are $\geq -1$. We can see that these singularities are all log terminal but not canonical (indeed, canonical surface singularities are precisely the ADE singularities; there are no nonsmooth terminal surface singularities).

## A.2 Is it a P-resolution or not?

Recall that a partial resolution $g\colon Z \to \mathbf{C}^2/G$ of a cyclic quotient singularity is called a P-resolution if it has at worst T-singularities and if $K_Z \cdot D > 0$ for any curve $D \subset Z$ contracted by $g$. Let $f\colon Y \to Z$ be a resolution of singularities of $Z$. Let $\cup_i E_i$ be the exceptional locus of $f$ and let $k_i$ be the discrepancies (so $K_Y = f^* K_Z + \sum k_i E_i$). If $D \subset Z$ is an irreducible curve then there is a unique irreducible curve $C \subset Y$ such that $f_* C = D$. We have

$$K_Z \cdot D = f^* K_Z \cdot C = (K_Y - \sum k_i E_i) \cdot C.$$

**Example A.4.** Suppose that $Y$ is the minimal resolution of $\frac{1}{11}(1,3)$ (which contains $C_1, C_2$ with $C_1^2 = -4$, $C_2^2 = -3$) and $Z$ is obtained from $Y$ by collapsing $C_1$. We have

$$K_Z \cdot f_* C_2 = K_Y \cdot C_2 - (-1/2) C_1 \cdot C_2.$$

Since $K_Y \cdot C_2 = -C_2^2 - 2 = 1$ and $C_1 \cdot C_2 = 1$, this gives

$$K_Z \cdot f_* C_2 = \frac{3}{2} > 0,$$

which shows that $f\colon Y \to Z$ is a P-resolution.

**Exercise A.5.** Consider the chain $C_1, C_2$ with $C_1^2 = -4$, $C_2^2 = -3$ again. Blow up a point on $C_1$ and a point on the exceptional curve of this blow-up to obtain a surface $Y'$ with a chain of spheres $E_1, E_2, E_3, E_4$ with $E_1^2 = -1$, $E_2^2 = -2$, $E_3^2 = -5$, $E_4^2 = -3$. Collapse $E_2, E_3, E_4$ to obtain a surface $Z'$ with a $\frac{1}{25}(1, 14)$ singularity (because $2 - \frac{1}{5-\frac{1}{3}} = \frac{25}{14}$). Show that $K_{Z'} \cdot (f')_* E_1$ is negative, so that this is not a P-resolution of $\frac{1}{11}(1, 3)$. [I get $K_{Z'} \cdot (f')_* E_1 = -3/5$.]

## A.3 Enumerating P-resolutions

Kollár and Shepherd-Barron show [11, Lemma 3.13] that any P-resolution of $\frac{1}{n}(1, a)$ is obtained from a certain "maximal resolution" by contracting some curves to get T-singularities (equivalently, the smoothing is obtained by rationally blowing down some chains of curves in the maximal resolution). Since there is a finite number of curves to contract/rationally blow-down, this shows there are only finitely many P-resolutions.

Rather than explaining their proof, I will just describe how to find the maximal resolution. Let $X$ be the cyclic quotient singularity. Let's define a poset whose elements are resolutions $f\colon Y \to X$ obtained by blowing up intersections between exceptional curves of the minimal resolution and where $Y_1 < Y_2$ if the resolution $f_2\colon Y_2 \to X$ factors through a morphism $Y_2 \to Y_1$. For any $Y$ in our poset, we have $K_Y = \sum(\alpha_j(Y) - 1)E_j$ for some $\alpha_j(Y) \in \mathbf{Q}$. If $Y_1 < Y_2$ then $\max_j \alpha_j(Y_1) > \max_j \alpha_j(Y_2)$ (i.e. as you move up in the poset, the number $\max_j \alpha_j(Y)$ increases). The maximal resolution is defined to be the maximal element in the poset for which $\max_j \alpha_j(Y) < 1$.

**Example A.6.** Consider the case $n = 11, a = 3$. The minimal resolution is a chain of spheres $C_1, C_2$ with self-intersections $-4, -3$. Blow up the unique intersection point to obtain a $-1$-sphere $E$ (and continue to write $C_1, C_2$ for the proper transforms of $C_1, C_2$). We can compute that

$$K = -\frac{7}{11}C_1 - \frac{2}{11}E - \frac{6}{11}C_2,$$

giving $\alpha_1 = 4/11$, $\alpha_2 = 9/11$, $\alpha_3 = 5/11$. If we blow-up the point $C_1 \cap E$ then we get $\alpha_2 = 13/11 > 1$ (for the new exceptional sphere). If we blow-up the point $C_2 \cap E$ then we get $\alpha_3 = 14/11 > 1$ (for the new exceptional sphere). So the maximal resolution is the one-point blow-up of the minimal resolution. This has a chain of three spheres with self-intersections $-5, -1, -4$. We can collapse the $-4$-curve to get a surface with a T-singularity (this is a P-resolution of $\frac{1}{11}(1, 3)$). We can collapse the $-1$ curve and then the $-4$ curve to get a surface with a T-singularity (this is another P-resolution). This exhausts the possible P-resolutions.

**Exercise A.7.** Work through the example of $\frac{1}{19}(1, 7)$ ([11, Example 3.15]) which I discussed in Example 2.15.

# References


[1] D. Auroux. Mirror symmetry and T-duality in the complement of an anti-canonical divisor. *Journal of Gökova Geometry Topology*, 1:51–91, 2007.

[2] K. Cieliebak and Ya. Eliashberg. *From Stein to Weinstein and back*, volume 59 of *American Mathematical Society Colloquium Publications*. American Mathematical Society, Providence, RI, 2012. Symplectic geometry of affine complex manifolds.

[3] T. Delzant. Hamiltoniens périodiques et images convexes de l'application moment. *Bull. Soc. Math. France*, 116(3):315–339, 1988.

[4] J. J. Duistermaat. On global action-angle coordinates. *Comm. Pure Appl. Math.*, 33(6):687–706, 1980.

[5] J. D. Evans and I. Smith. Bounds on Wahl singularities from symplectic topology. *arXiv:1708.02268, to appear in Algebraic Geometry*, 2017.

[6] J. D. Evans and I. Smith. Markov numbers and Lagrangian cell complexes in the complex projective plane. *Geom. Topol.*, 22(2):1143–1180, 2018.

[7] J. D. Evans and G. Urzúa. Antiflips, mutations, and unbounded symplectic embeddings of rational homology balls. *arXiv:1807.0607*, 2018.

[8] P. Hacking and Yu. Prokhorov. Degenerations of Del Pezzo surfaces I. *arXiv:0509529*, 2005.

[9] P. Hacking and Yu. Prokhorov. Smoothable del Pezzo surfaces with quotient singularities. *Compositio Mathematica*, 146(1):169–192, 2010.

[10] P. Hacking, J. Tevelev, and G. Urzúa. Flipping surfaces. *J. Algebraic Geom.*, 26(2):279–345, 2017.

[11] J. Kollár and N. I. Shepherd-Barron. Threefolds and deformations of surface singularities. *Invent. Math.*, 91(2):299–338, 1988.

[12] P. Lisca. On symplectic fillings of lens spaces. *Transactions of the American Mathematical Society*, 360:765–799, 2008.

[13] D. McDuff and D. Salamon. *Introduction to symplectic topology*. Oxford University Press, second edition, 2005.

[14] A. Némethi and P. Popescu-Pampu. On the Milnor fibers of cyclic quotient singularities. *Proceedings of the London Mathematical Society*, 101(3):554–588, 2010.

[15] J. Rana. A boundary divisor in the moduli spaces of stable quintic surfaces. *Internat. J. Math.*, 28(4):1750021, 61, 2017.

[16] J. Rana and G. Urzúa. Bounding T-singularities on KSBA surfaces. *Advances in Mathematics*, 345:814–844, 2019.

[17] M. Symington. Four dimensions from two in symplectic topology. In *Topology and geometry of manifolds (Athens, GA, 2001)*, volume 71 of *Proc. Sympos. Pure Math.*, pages 153–208. Amer. Math. Soc., Providence, RI, 2003.

[18] N. T. Zung. Symplectic topology of integrable Hamiltonian systems, II: topological classification. *Compositio Mathematica*, 138(2):125–156, 2003.